CHEMICALLY DEPOSITED NANOCRYSTALLINE THIN FILMS AND THEIR APPLICATIONS

B. H. Patil and C. D. Lokhande
Thin Film Physics Laboratory, Department of Physics,
Shivaji University, Kolhapur- 416 004 (M. S.) India.
* Corresponding author Tel. +91 231 2609225, Fax: +91 231 26092333.
E-mail: l_chandrakant@yahoo.com (Prof. C. D. Lokhande)

Abstract

Currently, there is a great interest in the methods of creating nanostructured materials with high performance nano-devices for the solar cell, dye-sensitized solar cells (DSSC), gassensor and supercapacitor applications. The systematic studies on the preparation of nanostructured metal oxide as well as polyaniline based heterojunction thin films by using chemical/electrochemical reactions from aqueous solutions for solar cell, DSSC, gas sensor and supercapacitor applications is explored. This paper includes the different deposition methods such as chemical bath deposition (CBD), successive ionic adsorption and reaction (SILAR), spray pyrolysis (SP) and electrodeposition (ED) for the deposition of nanostructured metal oxide and polyaniline based heterojunction thin films from aqueous solutions. Finally, the applications of thin films in solar cells, dye-sensitized solar cells (DSSC), gas sensing and supercapacitive performance of various materials such as ZnO, TiO2, NiO, RuO2, MnO2, SnO2, polyaniline, etc. and p-polyaniline/n-TiO2, p-polyaniline/n-ZnO, n-cadmium chalcogenide/p-polyaniline heterojunctions are discussed.

Keywords : Nanocrystalline, thin film, dye sensitized solar cell, supercapacitor, gas sensor.

1. Introduction

There has been increasing interest during the past few decades in semiconducting thin films because of their wide application in various fields of science and technology, leading to a drastic cut in the cost of production of semiconductor devices [1]. Thin films are of particular interest for the fabrication of large area photodiode arrays, solar selective coatings, solar cells, photoconductors, sensors, supercapacitors, etc. Deposition of films by vacuum evaporation, sputtering and chemical methods such as chemical bath deposition (CBD), spray pyrolysis, electrodeposition (ED), successive ionic adsorption and reaction (SILAR) methods are well known [2]. The chemical deposition route is attracting considerable attention as it is relatively inexpensive, simple and convenient for large area deposition. It is a slow process which facilitates better orientation of crystallites with improved grain structure [3]. Depending upon the deposition conditions such as the bath temperature, stirring rate, pH, solution concentration, etc., the film growth can take place by ion-by-ion condensation on the substrates or by adsorption of the colloidal particles from the solution onto a substrate [2]. Using chemical deposition, thin films of the compounds II-VI, IV-VII, V-VI and I-III-VI etc. have been deposited. The range of thin film application is very large and extends from micrometer dots in microelectronics to coatings of several square meters on window glasses. Dictated by considerations of simplicity, economics end input energy, large area thin films necessarily have to be deposited by chemical techniques [4]. It does not require sophisticated instrumentation like vacuum systems end other expensive equipment. It can be carried out in a glass beaker and a hot plate and a stirrer are the equipment needed. The starting chemicals are commonly available and cheap materials. With chemical depositions a large number of substrates can be coated in a single run with a proper jig design. Unlike in ED, electrical conductivity of the

substrate is not a necessary requirement in chemical deposition. Hence, any insoluble surface to which the solution has free access will be a suitable substrate for deposition [5]. The low temperature deposition avoids oxidation or corrosion of metallic substrates. Chemical deposition results in pinhole free and uniform deposits as the solution from which these are deposited always remains in touch with the substrates, since the basic building blocks are ions instead of atoms [2]. The preparative parameters are easily controllable and better orientation and improved grain structure can be obtained. The process of precipitation of a substance from the solution onto a substrate depends mainly on the formation of a nucleus and subsequent growth of a film. Using chemical deposition, a number of binaries, such as CdSe, Bi2S3, Bi2Se3, PbS, PbSe, Ag2S, TiSe, MoS2, ZnS, SnSe, etc. and ternaries such as CuInS2, CuZnSe2. CdnS, PbHgS, CdSe, etc. have been deposited as thin films.

In the present short review, the summary of our research work is discussed. Here, the thin films of metal oxides, conducting polymers are prepared by simple and cost effective chemical deposition techniques for different applications such as photoelctrochemical cell, DSSC, supercapacitor and gas sensor. Figure 1 shows the different inexpensive chemical deposition techniques.

2 Deposition of thin films by various chemical methods

2.1 Thin films by chemical bath deposition (CBD) method

Kale et al [6] reported the hexagonal transformation of surface morphology of CBD deposited CdSe thin film after annealing. Similarly, PbSe thin films were also synthesized at room temperature by CBD method using Pb(CH3COO)2, 25% NH4OH and freshly prepared Na2SeSO3 solutions as precursor. Fig.2 (A-B) shows the XRD pattern and SEM image of PbSe thin film deposited by CBD method [7].

Metal oxides are easily deposited by chemical method. TiO2 thin films grown onto ITO coated glass substrates using room temperature chemical deposition method from TiCl3 solution. The samples obtained are well adherent and amorphous in nature. Fig.3 (A-B) shows the XRD and SEM image of TiO2 thin film [8]. Shinde et al [9] deposited the hydrophobic and textured ZnO films by CBD method. They also studied the effect of annealing on their physic-chemical properties of ZnO film. Warm like nickel oxide [10], porous nanograins of polyaniline and interlocked cubes of Mn_3O_4 [11] are also obtained by CBD method.

In our laboratory, we have deposited thin films of binary sulphites (CdS, ZnS, Bi2S3, Sb2S3, As2S3, PbS, HgS,, MnS, Cu_xS, Ag2S, SnS, SnS2, In2S3, FeS2, NiS), Ternary Sulphides (CdCr2S4, HgCr2S4, HgCdS. CdZnS, CdSSe, CuInS2), binary and ternary selenides (CdSe, ZnSe, HgSe, PbSe, Bi2Se3, Sb2Se3, CuSe, InSe, CuInSe2), metal oxides (ZnO, Bi2O3, CdO, CuO, MnO2, TiO2, Co3O4, NiO, RuO2, NiFe2O4, In2O3, Fe2O3) and conducting polymers (polyaniline, polypyrrole) by CBD method.

2.2 **Thin films by Successive ionic layer adsorption and reaction (SILAR) method**

Kale et al [12] deposited TiO2 by simple chemical method called SILAR by alternate immersion of substrates in Ti^{4+} source and double distilled water precursor solutions maintained at 333 K, The pH of the solution is adjusted at 3–4. The oxygen precursor is the double distilled water maintained at temperature of 333 K. Uniform and well adherent ZnO thin films are also deposited by SILAR method [13]. Fibrous nanorod network is observed for SILAR deposited Bi2O3 thin films as shown in Fig. 4 [14]. Different selenides such as CdSe [15], InSe [16] and CuSe [17] are also deposited by SILAR method on glass as well as stainless substrates. The surface morphology of these films is shown in below Fig. 5.

Ternary compounds such as CuInS2 [17] and CuInSe2 [18] are also deposited by SILAR method. Further, these films used for the solar cell application.

2.3 Thin films by electrodeposition (ED) method

The electrochemical process is used for the deposition of nanocrystalline cobalt and nickel ferrites having high porosity [19, 20]. Fig. 6 shows the SEM images of electrodeposited Bi2O3, Fe_2O_3 and BiFeO3. The conducting polymer such as polyaniline is easily deposited by electrodeposition with nanofibrillar surface morphology [21].

2.4 Thin films by spray pyrolysis method

Nanobeads are observed for the spray deposited ZnO thin films. Interconnected web-like architecture growth of sprayed TiO2 films is reported by More et al [22].

3.Applications of chemically deposited thin films

The thin films of metal oxides and conducting polymers deposited by chemical method are used for the applications of solid state solar cells, photoelectrochemical cells, dye-sensitized solar cells, supercapacitors, buffer layers and gas sensors.

Nanofibrillar CdSe shows the 2% photo conversion efficiency [23]. Whereas, the dye sensitized solar cells are fabricated using TiO2, ZnO, CdO,TiO2/CdSe etc. Using TiO2 and ZnO thin films, the dye synthesized solar cells with conversion efficiency of 4.5% has been reported [24]. Fig. 7 shows the (a) schematic diagram of dye sensitized solar cell and (b) photograph of dye synthesized solar cell with rose bengal dye. Mane et al [25] obtained the highest efficiency about 2.2 1% for ZnO thin film. Fig. 8 shows the I-V characteristics of ZnO electrodes at different thickness. 2.95% conversion efficiency is obtained for CdO based dye sensitized solar cell in N3 dye [26].

Chemically deposited β-Ni(OH)2 shows the interconnected mesoporous honeycomb like structure. The maximum value of specific capacitance about 398 $F.g^{-1}$ is obtained for Ni(OH)2thin films in 2M KOH electrolyte [27]. Whereas, electrochemically deposited Co(OH)2 shows the specific capacitance about 260 $F.g^{-1}$[28]. Dhawale et al [29] obtained the maximum value of specific capacitance (925 $F.g^{-1}$) for galvanostatically deposited polyaniline thin films than potentiostatic (861 $F.g^{-1}$) and potentidyanamically (758 $F.g^{-1}$) deposited thin films. Metal oxide such as MnO2 is the effective material for supercapacitor application. Dubal et al [30] observed that, with cycling of Mn_3O_4 the morphology changes (Fig. 9) and Mn_3O_4 is converted into MnO2after 3000 cycles with 85% cyclic stability over 5000 cycles (Fig. 9).

Multilayer nanosheets of Cu2O are obtained by chemical method. Cu2O electrode shows the specific capacitance about 43 $F.g^{-1}$ [31]. Conducting polymer such as polyaniline, polypyrrole and polythiophene are used as electrode material in supercapacitor. Nanograined polyaniline gives the specific capacitance about 839 $F.g^{-1}$ with 85 % cycling stability over 10000 cycles. Table 1 shows the supercapacitive materials deposited by chemical method with their specific capacitance values.

LPG sensors have been developed using chemically deposited ZnO, CdO, NiFe2O4, NiO, TiO2, etc. thin films. LPG consists of CH4, C_3H_8, and C_4H_{10}, etc. and in these molecules the reducing hydrogen species are bound to carbon atoms. Therefore, LPG dissociates less easily into reactive reducing components on the film surface. The overall reaction of LPG molecules with adsorbed oxygen can be explained as follows:

where C_nH_{2n+2} represents the CH4, C_3H_{10} and C4H10

The maximum sensitivity of 43% at the operation temperature of 673K to 0.4 vol.% LPG is reported by Shinde et al [32] for ZnO thin films (Fig.10).

Gunjakar et al [33] observed that the gas response increases from 30% to 37% for nickel oxide LPG sensor when it undergo the Pd sensitization. The effect of Pd sensitization on the sensing performance of CdO is also observed [34]. Spray deposited TiO2 is also used for the LPG gas sensor [35] with sensitivity about 35%. The gas sensing performance of hetrojuntions such as of p-polyaniline/n-TiO2 [36], p-polyaniline/n-ZnO [37], etc. are also testes. Table 2 shows the gas sensing properties of different materials deposited by chemical method.

4. Conclusions

The naocrystalline thin films of ZnO, Bi2O3, MnO2, CdO, TiO2, La2O3, Fe2O3, BiFeO3, Co3O4, Ferrites, polyaniline, polyaniline based heterojunctions, etc. have been deposited using inexpensive chemical methods**.** Further, these films are used in photoelectrochemical cells, dye sensitized solar cells, supercapacitors and gas sensor (LPG) applications.

References

[1] B. R. Sankapal, R. S. Mane, C. D. Lokhande, Mater. Res. Bull. 35 (2000)

2027.

[2] R. S. Mane, C. D. Lokhande, Mater. Chem. Phys. 65 (2000) 1.

[3] S. A. Vanalakar, S. S. Mali, M. P. Suryavanshi, P. S. Patil, J. Nanomaters. Biostru. 5 (2010) 805.

[4] R. R. Ahire, B.R. Sankapal, C.D. Lokhande, Mater. Res. Bull. 36 (2001) 199.

[5] S. D. Sartale, C.D. Lokhande, Ceram Int. 28 (2002) 467.

[6] R. B. Kale, C. D. Lokhande, J. Phys. Chem. B 109 (2005) 20288

[7] R. B. Kale, S. D. Sartale, V. Ganesan, C. D. Lokhande, Y. F. Lin, S. Y. Lu, Appl. Surf. Sci. 253 (2006) 930.

[8] C. D. Lokhande, E. H. Lee, K. D. Jung, O. S. Joo, J. Mater. Sci. 39 (2004) 2915.

[9] V. R. Shinde, C. D. Lokhande, R. S. Mane, S. H. Han, Appl. Surf. Sci. 245 (2005) 407.

[10] J. L. Gunjakar, A. M. More, C. D. Lokhande, Sens Actuators B 131 (2008) 356.

[11] D. P. Dubal, D. S. Dhawale, R. R. Salunkhe, S. M. Pawar, V. J. Fulari, C. D. Lokhande, J. Alloys Compd 484 (2009) 218.

[12] S. S. Kale, R. S. Mane, H. Chung, M. Y. Yoon, C. D. Lokhande, S. H. Han, Appl. Surf. Sci. 253 (2006) 421.

[13] C. D. Lokhande, H. M. Pathan, M. Giersig, H. Tributsch, Appl. Surf. Sci. 187 (2002) 101.

[14] T. P. Gujar, V. R. Shinde, C. D. Lokhande, S. H. Han, J. Power Sources, 161 (2006) 1479.

[15] H. M. Pathan, B. R. Sankapal, C. D. Lokhnde, Mater. Chem. Phys, 78 (2002) 11.

[16] H. M. Pathan, S. S. Kulkarni, S. H. Han, C. D. Lokhande, Mater. Res. Bull. 40 (2005) 1018.

[17] H. M. Pathan, C. D. Lokhande. Appl. Surf. Sci. 239 (2004) 11.

[18] H. M. Pathan, C. D. Lokhande, Appl. Surf. Sci. 245 (2005) 328.

[19] C. D. Lokhande, S. S. Kulkarni, R. S. Mane, K. C. Nandi, S. H. Han, Curr. Appl. Phys. 8 (2008) 612.

[20] C. D. Lokhande, S. S. Kulkarni, R. S. Mane, S. H. Han, J. Magn. Magn. Mater. 313 (2007) 69.

[21] S. S. Joshi, C. D. Lokhande, Appl. Surf. Sci. 252 (2006) 8539.

[22] A. M. More, J. L. Gunjakar, C. D. Lokhande, R. S. Mane, S. H. Han, Micron, 38 (2007) 500.

[23] S. K. Min, O. S. Joo, R. S. Mane, K. D. Jung, C. D. Lokhande, S. H. Han, J. Photochem. and Photobio. A: Chemistry 187 (2007) 133.

[24] R. S. Mane, S. J. Roh, C. D. Lokhande , S. H. Han, Appl. Phys. Letter. 25 (2007) 3512.

[25] R. S. Mane, W. J. Lee, C. D. Lokhande, B. W. Cho, S. H. Han, Curr. Appl. Phys. 8 (2008) 549.

[26] R. S. Mane, H. M. Pathan, C. D. Lokhande, Sung-Hwan Han, Sol. Energy Mater. Sol. Cells, 80 (2006) 185.

[27] U. M. Patil, V. J. Fulari, K. V. Gurav, C. D. Lokhande, O. S. Joo, J. Power Sources 188 (2009) 338.

[28] S. G. Kandalkar, J. L. Gunjakar, C. D. Lokhande, Appl. Surf. Sci. 254 (2008) 5540.

[29] D. S. Dhawale, R. R. Salunkhe, V. S. Jamadade, D. P. Dubal, S. M. Pawar, C. D. Lokhande, Curr. Appl. Phy. 10 (2010) 904.

[30] D. P. Dubal, D. S. Dhawale, R. R. Salunkhe, C. D. Lokhande, J. Electrochem. Soc. 157 (2010) A812.

[31] D. P. Dubal, D. S. Dhawale, R. R. Salunkhe, V. S. Jamdade, C. D. Lokhande, J. Alloys Compd. 492 (2010) 26.

[32] V. R. Shinde, T. P. Gujar, C. D. Lokhande, Sens. Actuators B, 123 (2007) 701.

[33] J. L. Gunjakar, A. M. More, C. D. Lokhande, Sens. Acturators B, 131 (2008) 356.

[34] R. R. Salunkhe, C. D. Lokhande Sens. Actuators B, 129 (2008) 345.

[35] A. M. More, J. L. Gunjakar, C. D. Lokhande, Sens. Actuators B, 129 (2008) 671.

[36] D. S. Dhawale, R. R. Salunkhe, U. M. Patil, K. V. Gurav, A. M. More, C. D. Lokhande, Sens Actuators B, 134 (2008) 988.

[37] D. S. Dhawale, C. D. Lokhande, J. Alloys Compd. 509 (2011) 10092.

Figure captions

Fig. 1 The various chemical deposition techniques (A) chemical bath deposition (B) successive ionic layer adsorption and reaction method (C) electrodeposition and (D) spray pyrolysis deposition.

Fig. 2 (A) XRD and (B) SEM image of chemically deposited PbSe thin film.

Fig. 3 (A) XRD and (B) SEM image of chemically deposited TiO_2 thin film.

Fig. 4 The SEM image of SILAR deposited $_{Bi2O3}$ thin film.

Fig. 5 The SEM images of (A) CdSe (B) InSe and (C) CuSe thin films.

Fig. 6 The SEM images of electrodeposited (A) $_{Bi2O3}$ $^{(B)}$ $_{Fe2O3}$ and (C) $BiFeO_3$ thin films.

Fig. 7 (a) Schematic diagram of dye sensitized solar cell and (b) Photograph of dye sensitized solar cell with rose Bengal dye.

Fig. 8 The I-V characteristics of ZnO electrodes at different thickness.

Fig. 9 The SEM images of $_{Mn3O4}$ with different cycling CV curves of (a-a') As prepared manganese oxide (b-b') After 1000 cycles (c-c') After 2000 cycles (d-d') After 3000 cycles.

Fig. 10 The effect of operating temperature on the LPG sensing performance of ZnO thin film.

Fig. 1

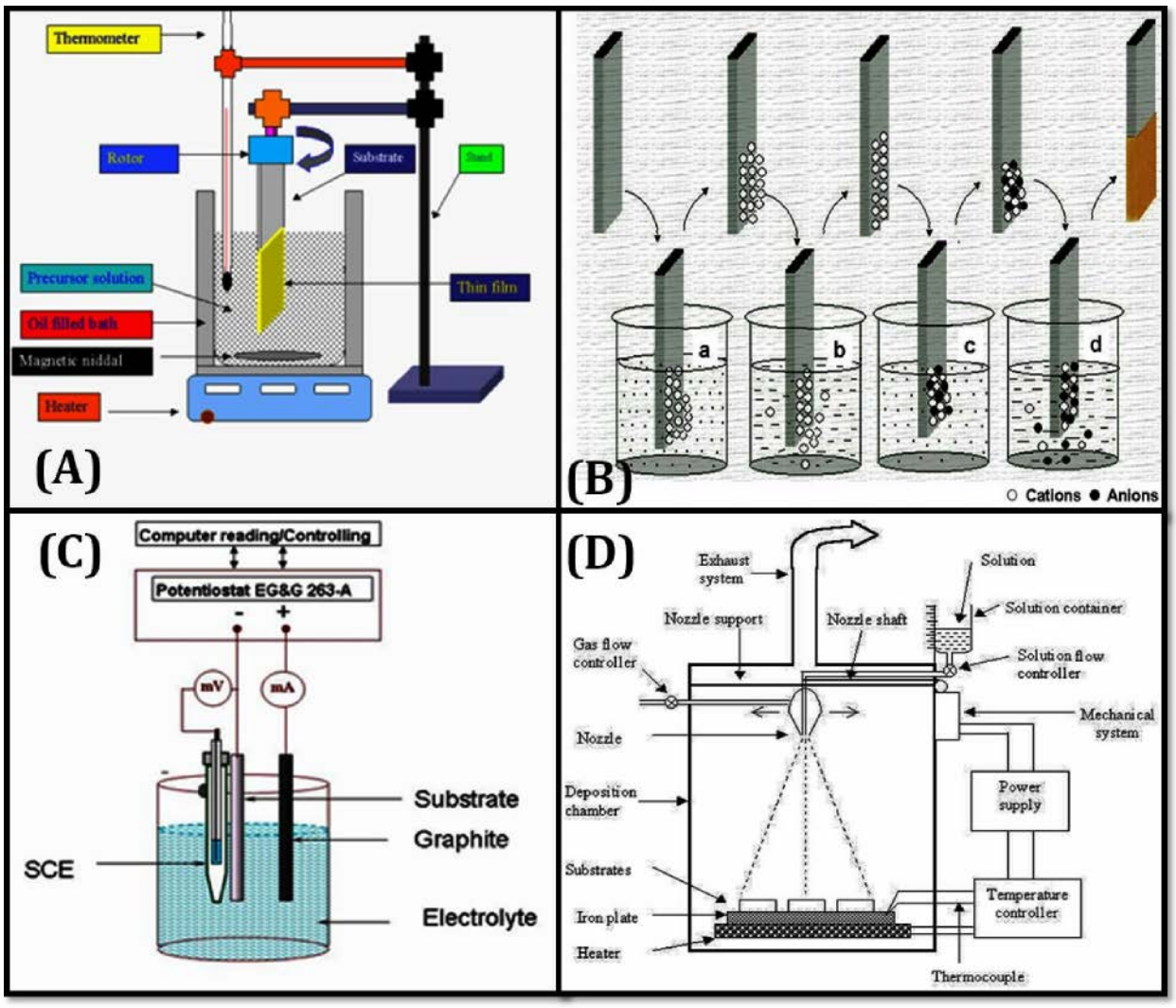
Thermometer
Rotor
Substrate
Precursor solution
Thin film
Oil filled bath
Magnetic riddal
Heater
(A)
a
b
c
d
(B)
Cations
Anions
(C)
Computer reading/Controlling
Potentiostat EG&G 263-A
mV
mA
Substrate
Graphite
SCE
Electrolyte
(D)
Exhaust system
Solution
Solution container
Nozzle support
Nozzle shaft
Gas flow controller
Solution flow controller
Mechanical system
Nozzle
Deposition chamber
Power supply
Substrates
Iron plate
Heater
Temperature controller
Thermocouple

Fig. 2

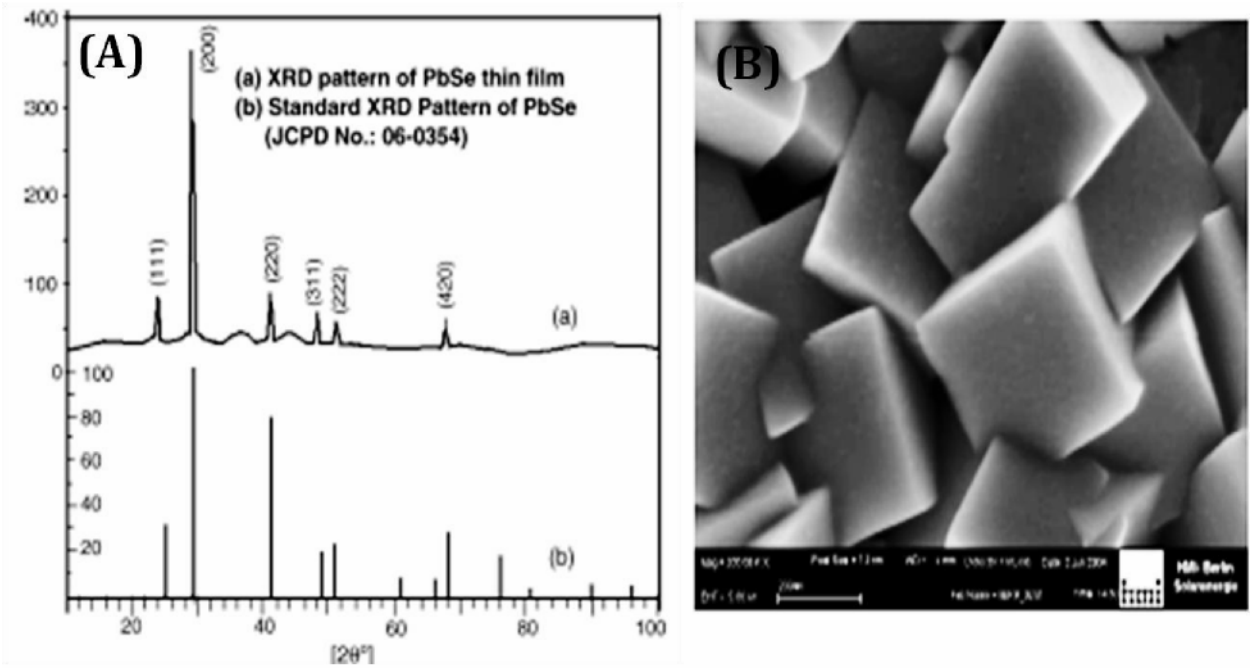
(A)
(a) XRD pattern of PbSe thin film
(b) Standard XRD Pattern of PbSe
(JCPD No.: 06-0354)
(111)
(200)
(220)
(311)
(222)
(420)
(a)
(b)
[2θ°]
(B)

Fig. 3

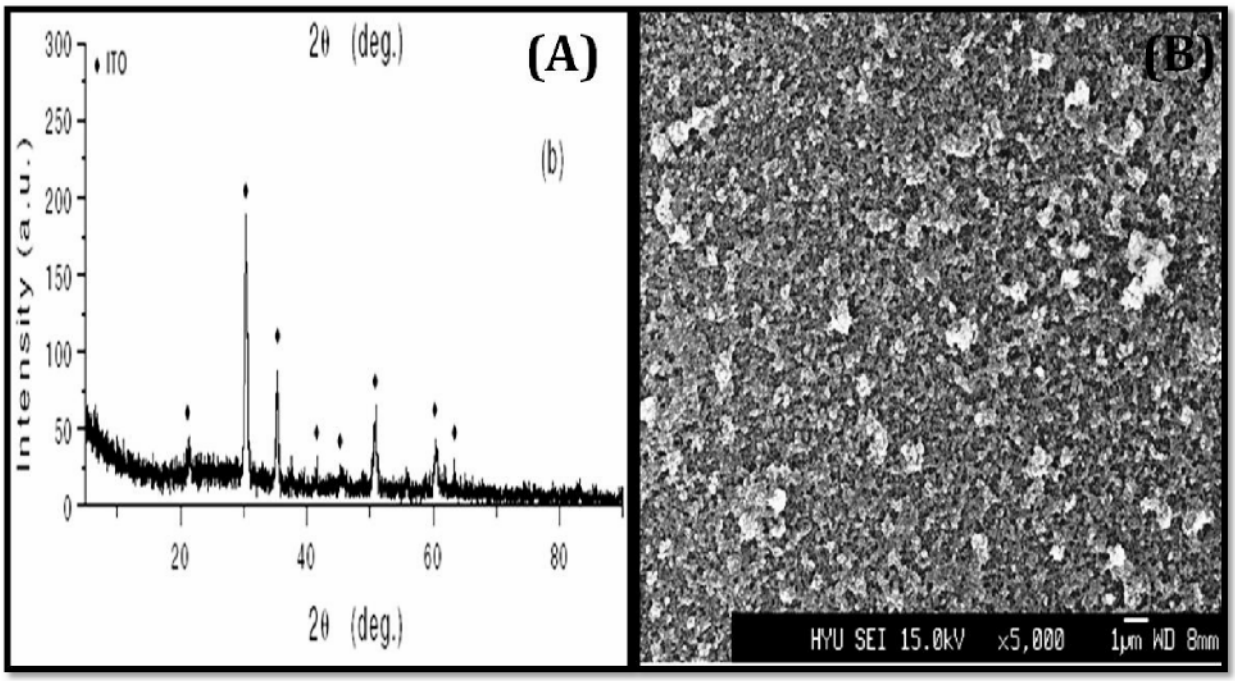
ITO
2θ (deg.)
(A)
(b)
Intensity (a.u.)
2θ (deg.)
(B)
HYU SEI 15.0kV x5,000 1μm WD 8mm

Fig. 4

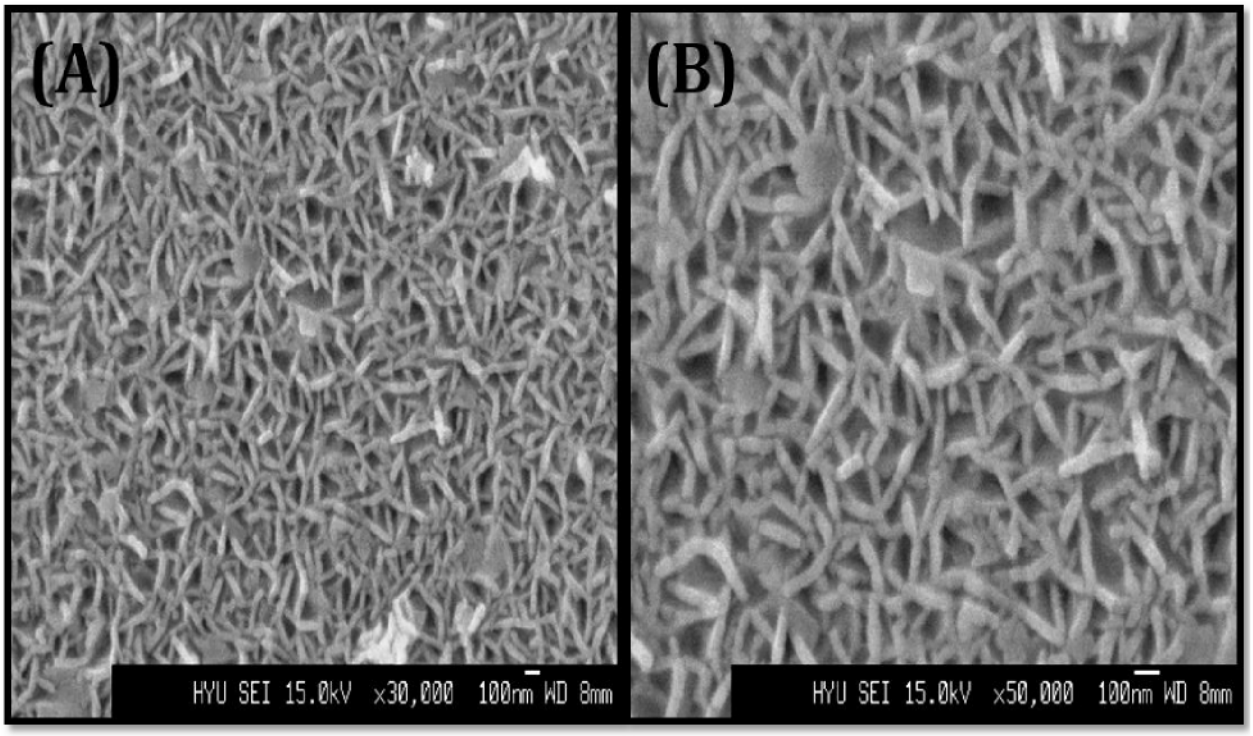
(A)
HYU SEI 15.0kV x30,000 100nm WD 8mm
(B)
HYU SEI 15.0kV x50,000 100nm WD 8mm

Fig. 5

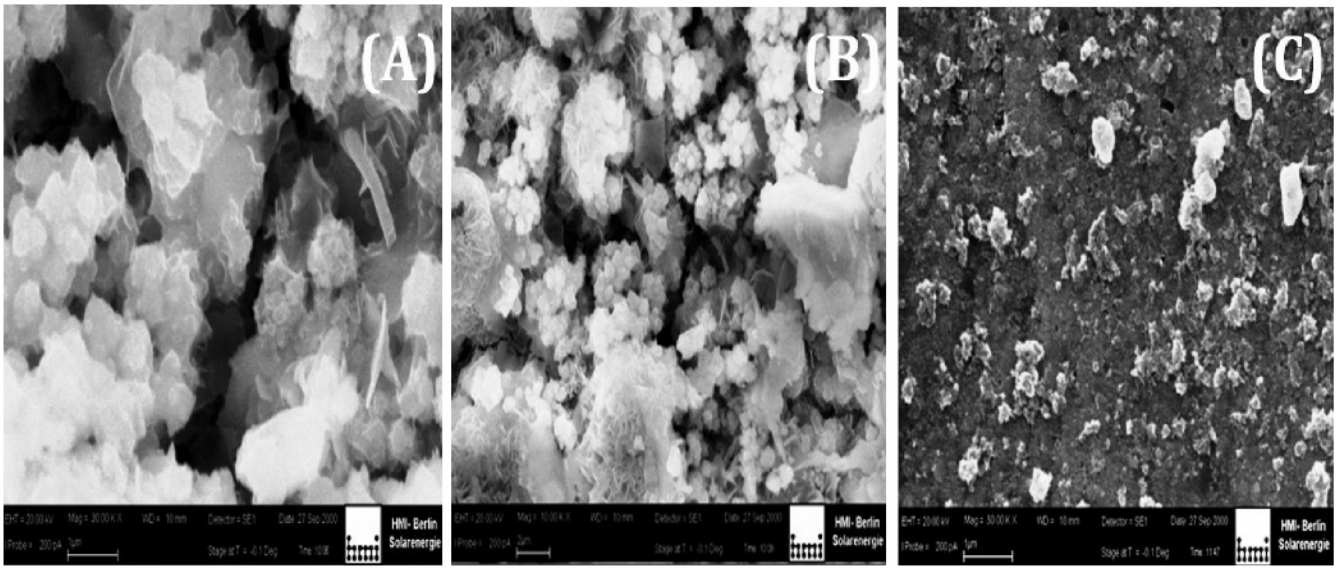
(A)
HMI- Berlin Solarenergie
(B)
HMI- Berlin Solarenergie
(C)
HMI- Berlin Solarenergie

Fig. 6

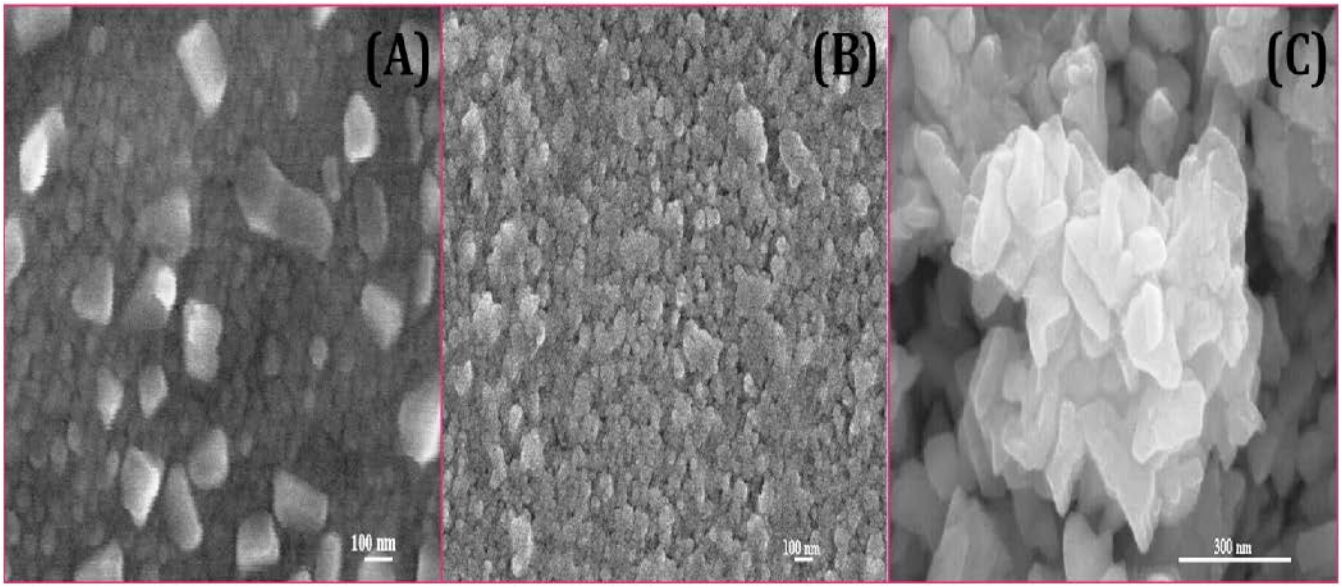
(A)
100 nm
(B)
100 nm
(C)
300 nm

Fig. 7

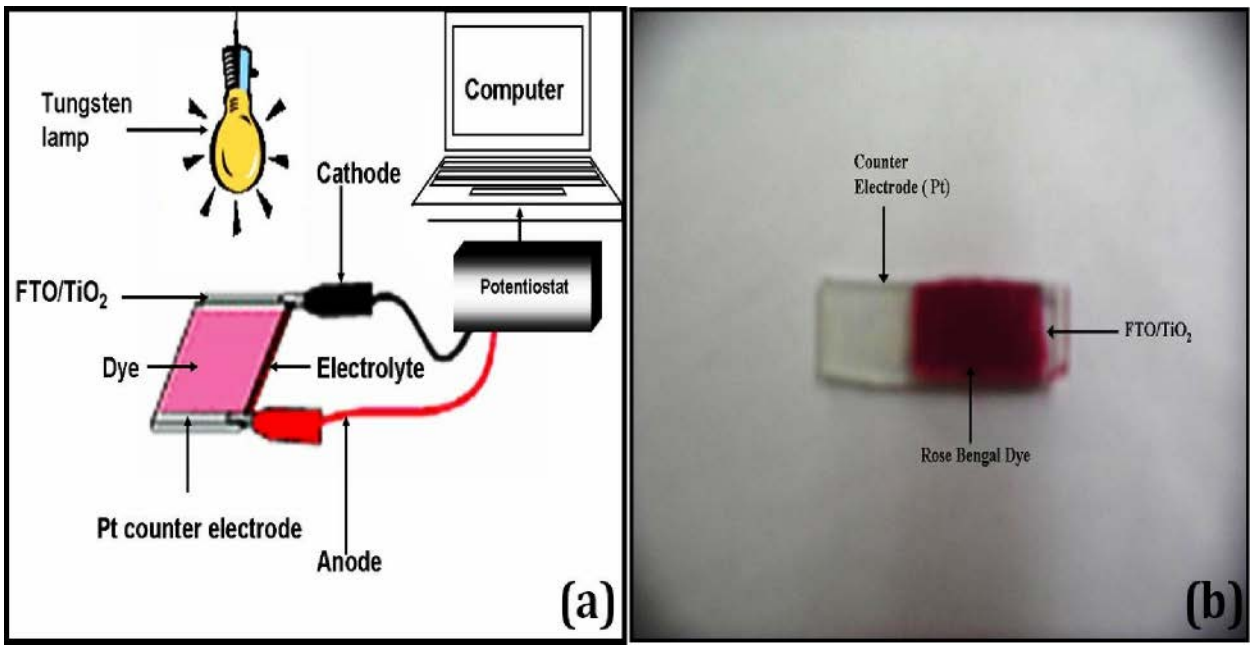
Tungsten lamp
Computer
Cathode
Potentiostat
FTO/TiO2
Dye
Electrolyte
Pt counter electrode
Anode
(a)
Counter Electrode (Pt)
FTO/TiO2
Rose Bengal Dye
(b)

Fig. 8

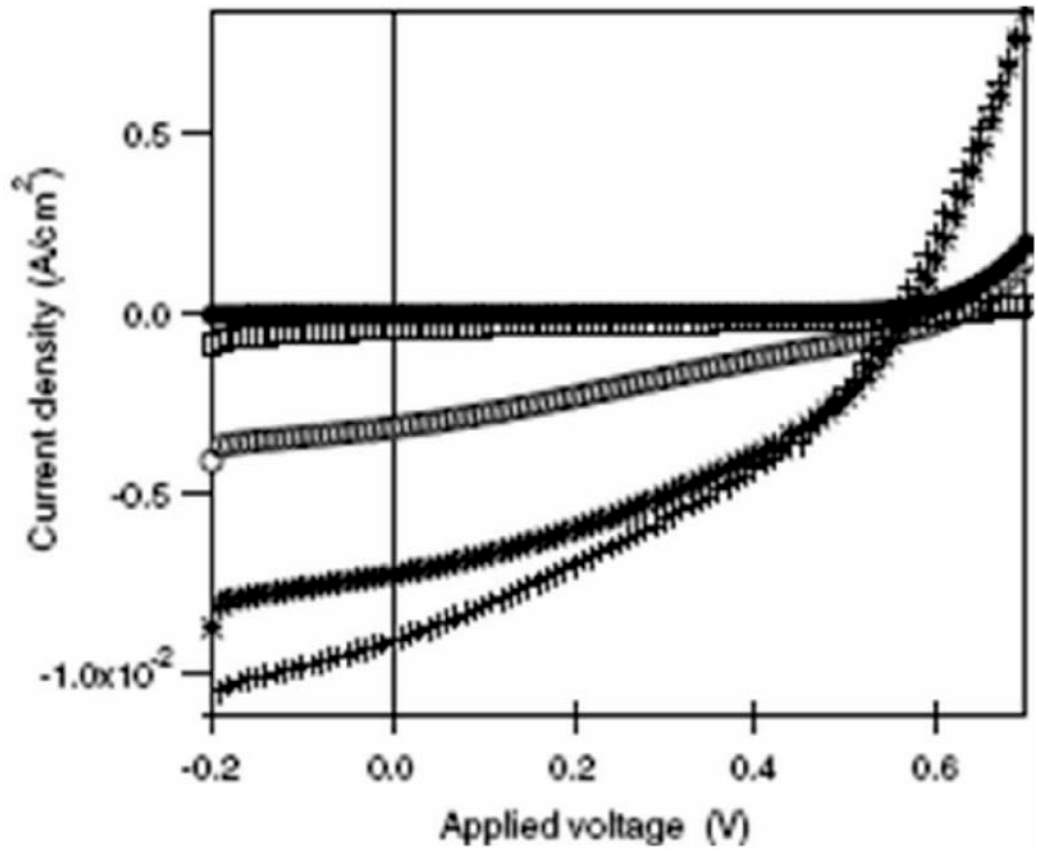
0.5
0.0
-0.5
-1.0x10^-2
Current density (A/cm^2)
-0.2
0.0
0.2
0.4
0.6
Applied voltage (V)

Fig. 9

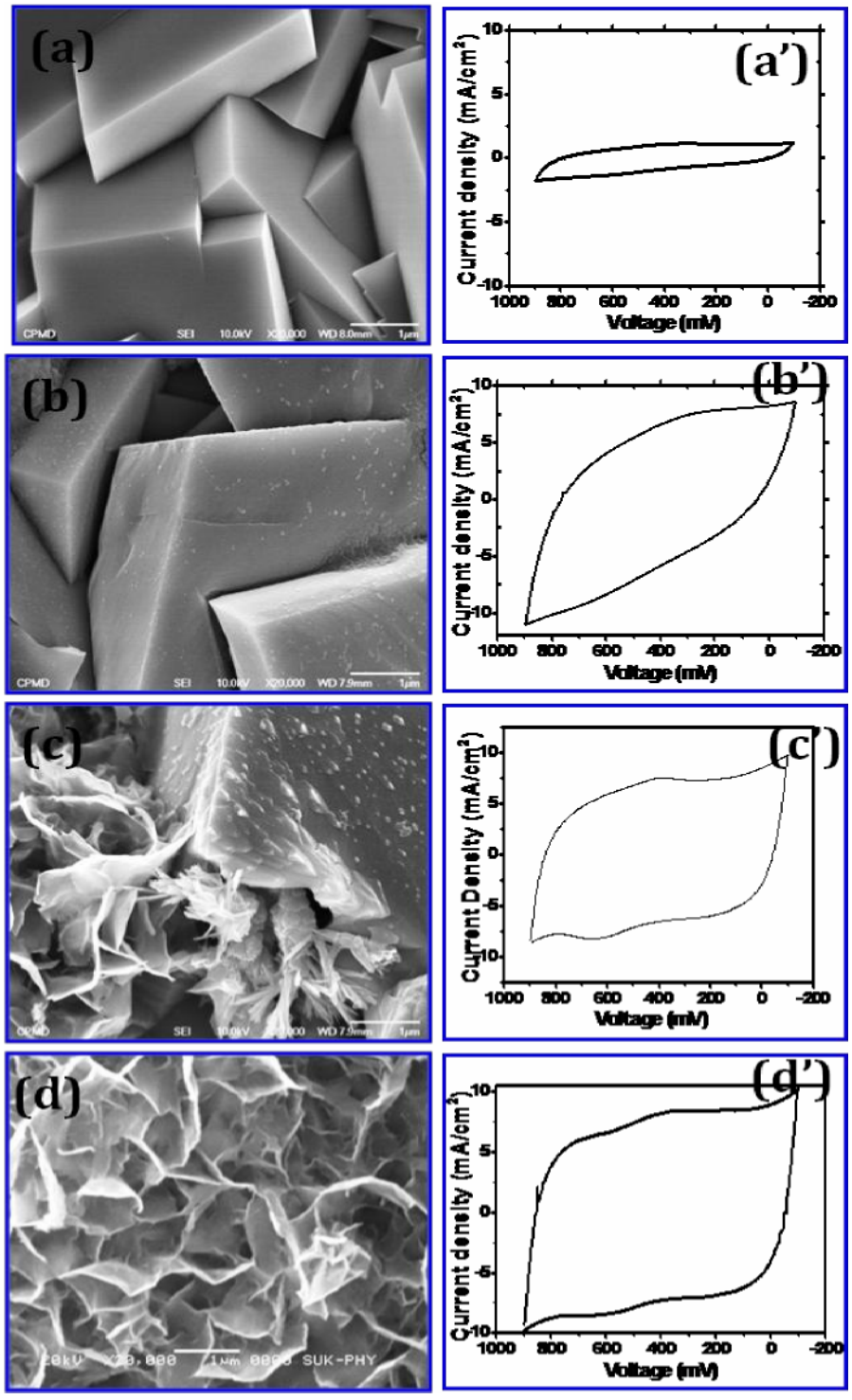
(a)
(a')
Current density (mA/cm²)
Voltage (mV)
(b)
(b')
Current density (mA/cm²)
Voltage (mV)
(c)
(c')
Current Density (mA/cm²)
Voltage (mV)
(d)
(d')
Current density (mA/cm²)
Voltage (mV)

Fig. 10

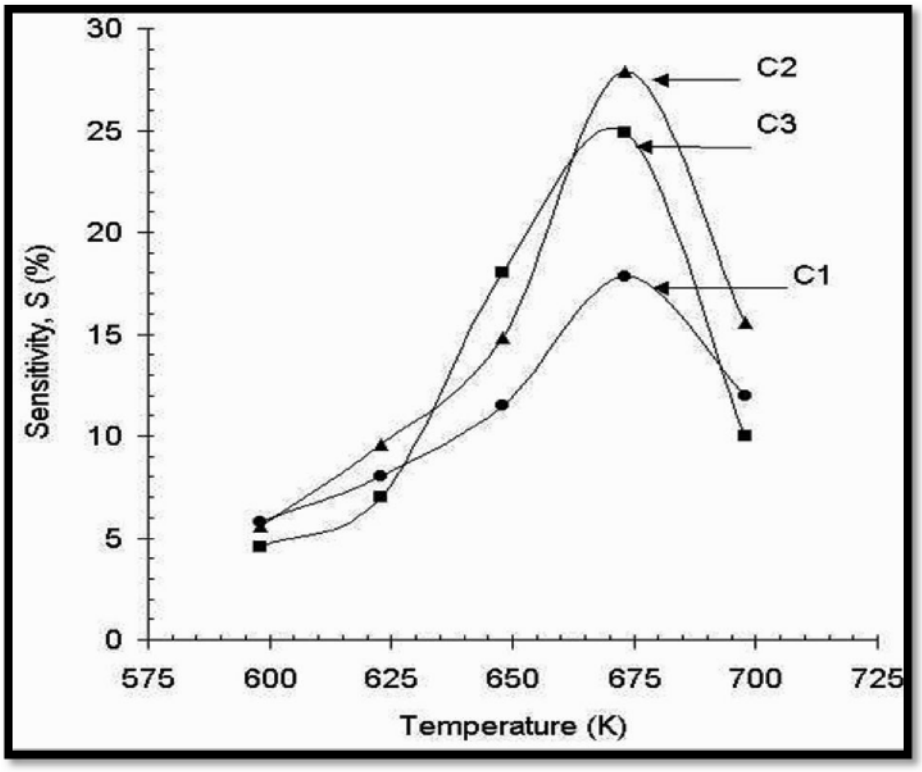
30
25
20
15
10
5
0
Sensitivity, S (%)
575
600
625
650
675
700
725
Temperature (K)
C2
C3
C1

Table 1 The chemically synthesized materials with their specific capacitance values.

Electrode	Electrolyte	Sp. Capacitance ($F.g^{-1}$)
CBD-CoO	KOH	118
CBD-Cu_2O	Na_2SO_4	43
CBD-NiO	KOH	169
CBD- $NiFe_2O_4$	Na_2SO_3	369
CBD-MnO_2	Na_2SO_4	223
CBD-Polyaniline	H_2SO_4	839
SILAR- MnO_2	Na_2SO_4	314
SILAR- $Ni(OH)_2$	KOH	350
SILAR- CoO	KOH	166
SILAR- RuO_2	H_2SO_4	50
SILAR-$NiFe_2O_4$	Na_2So_3	354
SILAR-Polyaniline	H_2SO_4	781
Spray- Co_3O_4	KOH	74
Spray- RuO_2	$H_2 SO_4$	551
ED-$CoFe_2O_4$	Na_2SO_3	81
ED- $NiFe_2O_4$	$Na_2 SO_3$	118

ED- RuO_2	H_2SO_4	788
ED- Bi_2O_3	NaOH	98
ED-$BiFeO_3$	NaOH	81
ED- Co_3O_4	KOH	185
ED- CoOOH	KOH	260
ED- Cu_2O	Na_2SO_3	36

Table 2 Gas sensing properties of different materials.

Sr. No.	Material	Deposition Technique	LPG Conc. (Vol %)	Temp. (K)	Gas Response (%)
1.	CdS/polyaniline	Electrodeposition	0.10	300	75
2.	CdSe/polyaniline	Electrodeposition	0.08	300	70
3.	CdTe/polyaniline	Electrodeposition	0.14	300	67.7
4.	TiO_2/polyaniline	CBD/ED	0.12	300	63
5.	ZnO/polyaniline	CBD/ED	0.10	300	81
5.	CdO	Spray Pyrolysis	0.16	698	38
6.	NiO	CBD	0.30	698	36.5

7.	TiO_2	Spray Pyrolysis	0.08	698	35.8
8.	Irradiated TiO_2	CBD	0.40	698	37
8.	Pd:CdO	Spray Pyrolysis	0.10	548	35
9.	CdO	CBD	0.16	698	23
10.	CdO	SILAR	0.10	698	18
11.	ZnO	CBD	0.20	627	75
12.	ZnO	Spray Pyrolysis	0.40	598	81